FLOMEKO 2022

Experimental Investigation on Measurement Characteristics of WMS for Gas-Liquid Slug Flow

Cenwei Sun[1], Ying Xu[1], Chao yuan[1], Tao Li[1], Huimin Ma[1], Yumeng Zhang[1], Xili Ba[2]

[1]Tianjin Key Laboratory of Process Measurement and Control, School of Electrical and Information Engineering, Tianjin University, suncw@tju.edu.cn, Tianjin, China
[2]PetroChina Planning & Engineering Institute, Beijing, China
E-mail (corresponding author): yuanchao@tju.edu.cn

Abstract

With the development of the gas-liquid two phase flow dynamics theory and the continuous improvement of two phase flowrate measurement requirements, the importance of slug flow research has become increasingly prominent. The wire mesh sensor (WMS), which consists of the perpendicular "cross-point" between the transmitting wires and receiving wires, forms a particular "hard field" measurement mode. This paper aims to investigate the measurement characteristics and accuracy of a 16×16-electrode conductivity WMS with a spatial resolution of 3.125mm for gas-liquid two phase slug flow by means of flow experiments. Experiments were performed in a 50 mm horizontal pipe with air and water as the working medium at atmospheric conditions, meanwhile, the time series data were collected by WMS. Comparing the cross sectional, a good correspondence can be found in the cross sectional direction between axial reconstructed images of fluid distribution and averaged void fraction time series. The WMS can realize the quantitative measurement of local void fraction and the qualitative spatial phase reconstruction of fluid distribution. Furthermore, distribution characteristics of the cross sectional averaged void fraction time series of gas-liquid two phase slug flow were analyzed. We found when superficial gas velocity is less than 3 m/s, the gas phase mainly exists in the form of elongate gas slug. When superficial gas velocity is around 5 m/s, it appears as typical bullet-shape gas slug. As superficial gas velocity increases to 10 m/s, the liquid slug becomes blurred and the gas phase almost penetrates through the liquid slug structures. In addition, a Probability Density Function (PDF) is generated from the instantaneous cross sectional averaged void fraction data for different flow regime conditions. The results show that the PDFs for lower superficial gas velocity case (3 m/s), two peaks in the void fraction signal are observed. Nevertheless, with an increase in superficial gas velocity, it is seen that the peak in the low void fraction region, which corresponds to the liquid slug structures, becomes much smaller even disappears.

1. Introduction

Gas-liquid slug flow is widely encountered in many practical industrial applications. It is very important to understand the flow characteristics of slug flow in detail. The wire mesh sensor (WMS) consists of the perpendicular "cross-point" between the transmitter wires and receiver wires. And the WMS forms a particular "hard field" measurement mode, which can realize the quantitative measurement of local void fraction and the qualitative spatial phase reconstruction of fluid distribution. According to the current received by the receiver wires, the conductivity or permittivity of the sensitive volume can be measured. Then the cross-sectional averaged void fraction and the reconstructed fluids distribution can be further derived [1]. The WMS [2-4] can also provide velocities, size and distributions of droplets/bubbles; interfacial area concentration; and capture complex fluid structures such as pseudo-slug flow [5] and fine gas-liquid interface [6]. WMS has been widely used because of its advantages such as high time-space resolution, simple image reconstruction algorithm and many measurable parameters.

As an intrusive instrument, WMS can cause some interference to the flows, so its measurement accuracy has also been widely concerned. S. Richte [7] and Weerin Wangjiraniran et al. [8] investigated the disturbance of WMS on flows by comparing the measurements of WMS and high-speed camera (HSC). Prasser [9] compared results of gas-liquid flow measured by X-ray CT with WMS in vertical pipeline, and the good agreements of phase distribution and void fraction can be obtained especially for big bubbles. Banowski [10] also investigate the measurement accuracy of WMS by systematically comparing the results of gas holdup and bubble size distribution obtained from the two technologies. Manera et al. [11] extracted some flow parameters of gas-liquid flows in vertical pipeline by WMS and conductance probe respectively, some of them are in good agreement, such as the relative errors of gas holdup, bubble velocity and phase interface concentration from the two technologies are 13%, 15% and 12%, respectively.

In this paper, the experiments of gas-liquid two-phase slug flow measured by WMS are carried out and corresponding time series data are collected. From this, the cross-sectional axial reconstructed images of fluid distribution and cross-sectional averaged void-fraction time series are obtained by calculation. Through systematically analyzing and comparing, there is a good correspondence with each other. This proves the excellent visualized merits of WMS and validates the feasibility of the coupling principle.

2. Sensor design and experiment setup

2.1 WMS measurement system

The schematic of the WMS is shown in Figure 1. As a visual means of flow observation, the WMS can reflect the spatial and temporal information for the gas–liquid distribution in the pipe. The WMS is designed in a 16*16 layout; therefore, the lateral resolution is 3.125 mm for the pipe diameter of 50 mm. To ensure good yield strength and tensile strength, both the transmitter and receiver electrodes are made of stainless steel. In addition, the diameter of all the electrodes is 0.1 mm, to minimize the damage to the flow field caused by the intrusion of the electrodes. The axial distance between the transmitter and receiver electrodes is 1.6 mm, and the excitation signal is bipolar square wave of 12 kHz, which effectively avoids the polarization phenomenon. During the period of one electrode excitation, the other excitation electrodes are grounded to prevent the mutual influence between different excitation electrodes. Through the NI USB-6210, the collected signals are imported into PC. Finally, the void fraction and the gas–liquid distribution imaging are obtained, where the imaging rate is 250 frames/second.

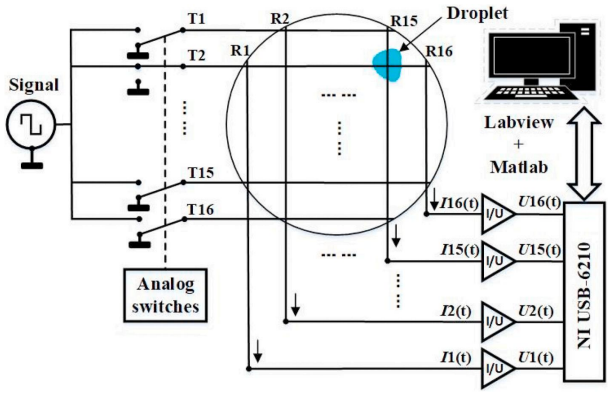

Figure 1: Schematic of the WMS

2.2 Experiment setup

The experiment of gas-water real flow measured by WMS was carried out on the adjustable medium pressure wet gas experimental facility of Tianjin University, which includes two loops of gas phase and liquid phase. This experiment only involved part of the pipeline with a diameter of 50 mm, as shown in Fig. 5. The gas-phase standard meter is turbine flowmeter (LWQ~1000, LWQ~400,1~400m3/h, U=0.35%, k=2). Electromagnetic flowmeter (AXF055g, AXF025g, 0.05~8m3/h, U=0.35%, k=2) is used for the liquid-phase standard meter.

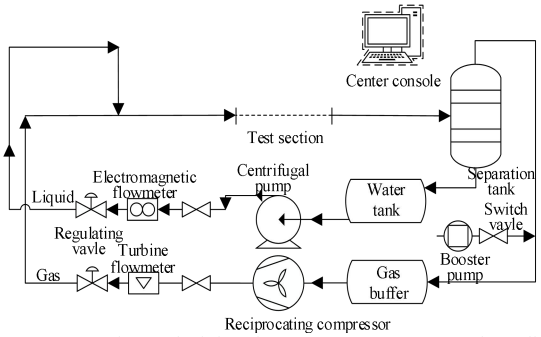

Figure 2: Experimental piping for WMS measurement of gas-liquid two-phase flow

The experiment was carried out under the condition of ambient temperature and atmospheric pressure (20℃±2℃, 101 kPa). The gas and liquid phase used in real flow experiment is air and tap water with electrical conductivity of 0.03 S/m and 0 S/m respectively. A 16×16 WMS with a resolution of 3.125 mm is used in the experiment. The data acquisition rate is 250 f/s, and the sampling time for each flow test point is about 60 s. This experiment involves stratified flow, wavy flow and slug flow. Details about superficial gas velocity (V_{SG}), superficial liquid velocity (V_{SL}) and liquid volume fraction (LVF) of each flow test point are shown in Table 1.

Table 1: Summary of the experiment conditions

V_{sg} (m/s)	*Vsl (m/s)*	*LVF (%)*
1	0.05, 0.11, 0.25, 0.43, 0.96	5, 10, 20, 30, 50
3	0.03, 0.093, 0.226, 0.529, 0.75, 1.286	1, 3, 7, 15, 20, 30
5	0.01, 0.015, 0.038, 0.051, 0.102, 0.155, 0.263, 0.376, 0.556, 0.882, 1.25	0.2, 0.3, 0.75, 1, 2, 3, 5, 7, 10, 15, 20
10	0.05, 0.1, 0.2, 0.31, 0.53, 0.75, 1.11, 1.50	0.5, 1, 2, 3, 5, 7, 10, 13
15	0.045, 0.075, 0.113, 0.152, 0.306, 0.464, 0.789, 1.129	0.3, 0.5, 0.75, 1, 2, 3, 5, 7
20	0.2, 0.62, 1.05	1, 3, 5

3. Experimental results

3.1 Normalized measurement of WMS

Research shows that the measurement of WMS has a positive relationship with the mixed conductivity of the fluids. Meanwhile, the relationship between the local mixed conductivity and the phase holdup in the same local area is generally assumed to be linear. Therefore, according to Equation (1), the local void fraction of fluid can be obtained by calibrating the direct measurement of WMS $U_{i,\,j,\,k}$ with measurement $U_{i,\,j}$, water under full-water condition, which also known as the normalized measurement of WMS.

$$\varphi_{i,\ j,\ k}=1-\frac{U_{i,\ j,\ k}}{U_{i,\ j,\ \text{water}}} \quad (1)$$

3.2 Reconstruction of fluid distribution and average void fraction

The cross-sectional average void fraction $\alpha_{g,\ aver}$ is derived from weighting local void fraction $\alpha_{g,\ k,\ i,\ j}$ summation:

$$\alpha_{g,\ aver,}=\sum_{i,j} a_{i,j}\cdot\alpha_{g,\ i,\ j} \quad (2)$$

The weight coefficient is determined by the area of each cross-point (*i, j*) of WMS accounted for the total area of measurement plane. In this paper, the weight coefficient is set as 1.

The reconstruction of fluid distribution along the axial direction of pipe contains 509 frames of WMS measurement data, i.e. it contains information about the time of 2.036 s. The reconstruction is obtained by mapping the normalized measurement of WMS to the different color grades. The red refers to the local void fraction of 1, representing the air. The blue refers to the local void fraction of 0, representing the water. And the fluid flows from the right to the left.

3.3 Results of slug flow

Figure 3, Figure 4 and Figure 5 respectively show the slug flow under the conditions of low gas velocity, medium gas velocity V_{sg} = 5 m/s and high gas velocity V_{sg} = 10 m/s. Due to the different gas and liquid velocity, the fluid structures of the slug flow corresponding to each flow point are different.

(1) Slug flow with low gas velocity

Figure 3 is the result of slug flow with low gas velocity and high liquid volume fraction, where the gas phase comes in the shape of long gas slug like elongated bubble. The gas slug flows along the top of the pipe. Besides each gas slug is segregated by liquid slug. The average void fraction corresponding to the gas slug is about 0.5, and the average void fraction corresponding to the liquid is about 0.1.

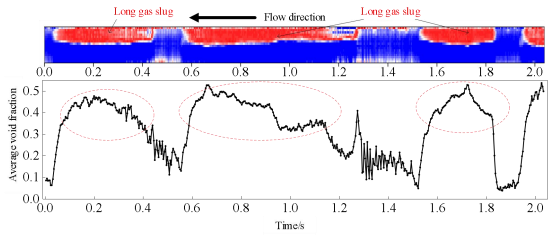

(a) V_{sg} = 1 m/s, Vsl = 0.96 m/s, LVF = 49%

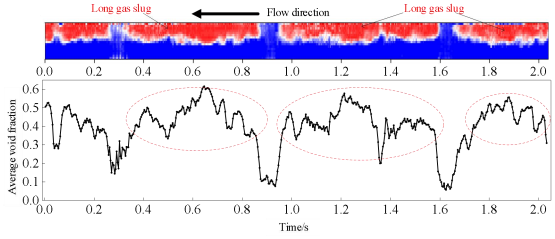

(b) V_{sg} = 3 m/s, Vsl = 1.296 m/s, LVF = 30%

Figure 3: Reconstruction images and time series of cross-sectional average void fraction for slug flow visualization under low air velocity conditions

The results (a) show that the average void fraction curve corresponding to the gas slug is smoother, and its fluctuation range and frequency are smaller than those of (b). It is because the superficial gas velocity of (a) is smaller than (b). In Figure 3, the gas slug moves slowly, and its gas-liquid interface is smooth. However, the gas slug of (b) moves faster. As a result, a small amount of liquid is entrapped in the gas slug, and the corresponding average void fraction has a larger fluctuation range.

(2) Slug flow with V_{sg} = 5 m/s

Figure 4 is the results of slug flow with V_{sg} = 5 m/s. The gas slug in Figure (a) and (b) both show a typical bullet shaped slug with a sharp head and a wide tail, which is obviously different from the long gas slug body. As shown in Figure (b), the length of gas slug is virtually the same, and the alternative flowing of the gas slug and the liquid slug present has a strong periodicity.

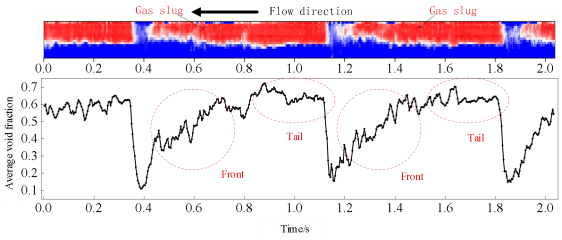

(a) V_{sg} = 5 m/s, Vsl = 0.88 m/s, LVF = 15%

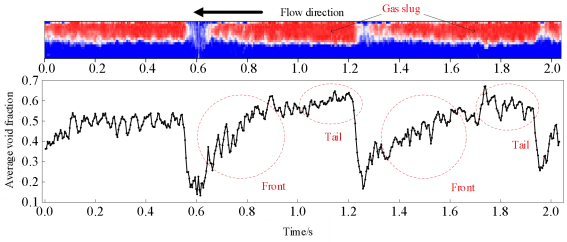

(b) V_{sg} = 5 m/s, Vsl = 1.25 m/s, LVF = 20%

Figure 4: Reconstruction images and time series of cross-sectional average void fraction for slug flow visualization under V_{sg} = 5 m/s

As shown in Figure 4, the region from the tail of the former gas slug to the head of the latter gas slug is completely filled with liquid, and the gas-liquid interface near the tail of the gas slug is relatively smooth, so the average void fraction corresponding to the tail rapidly decreases to 0.1. However, the average void fraction of the corresponding to the head of the gas slug increases slowly with a small fluctuation. As for the middle regions of the gas slug, the corresponding average void fraction tends to be stable at about 0.6. The trends of the average void fraction consist with the fluid distribution of slug flow.

(3) Slug flow with V_{sg} = 10 m/s

Figure 5 is the results of slug flow with V_{sg} = 10 m/s. As superficial gas velocity increase from V_{sg} = 5 m/s of Figure 4 to V_{sg} = 10 m/s of Figure 5, the profile of the gas slug has changed obviously. As shown in Figure (a),

the gas slug comes in the shape of a rugby ball with a sharper head and tail and a wider middle. Therefore, the average void fraction corresponding to the head and tail of the gas slug ramps slowly, meanwhile the average void fraction corresponding to the middle of the gas slug also fluctuates significantly. In addition, Figure (b) shows that most of the liquid plug become indistinct except for a few liquid plug which fills pipe. The average void fraction of the liquid slug is about 0.3, and it's indicated that liquid slugs of slug flow with V_{sg} = 10 m/s do not fill the entire pipe. In addition, compared with Figure 4, the periodic frequency increases but the length of the gas slug decreases with the increase of the superficial gas velocity.

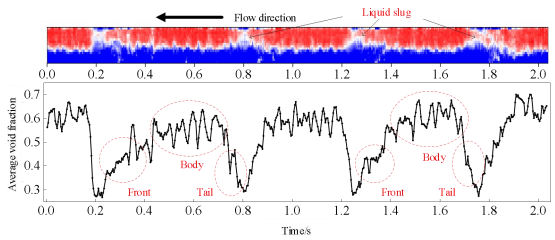

(a) V_{sg} = 10 m/s, Vsl = 1.11 m/s, LVF = 10%

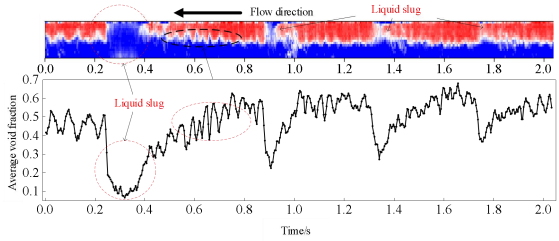

(b) V_{sg} = 10 m/s, Vsl = 1.49 m/s, LVF = 13%

Figure 5: Reconstruction images and time series of cross-sectional average void fraction for slug flow visualization under V_{sg} =10 m/s

As shown in Figure 3, 4 and 5, the superficial gas velocity of slug flow ranges from 1-10m/s, and the superficial liquid velocity is high, which ranges from 0.88-1.49m /s. With the increase of gas velocity, the fluid distribution comes in the form of long gas slug, bullet-shaped gas slug and slug flow with indistinct liquid slug. In fact, researches have shown that slug flow can be further subdivided into elongated bubble flow, bullet-shaped slug flow and pseudo-slug flow.

4. Distribution of void fraction

4.1 Time series of the cross-sectional average void fraction

As shown in Figure 6, the time series of the cross-sectional average void fraction of the slug flow presents a strong periodicity. For Figure (a) under the condition of low gas velocity, the high void fraction corresponds to the gas slug takes a huge part of time series curve. The results of Figure (b) with medium gas velocity V_{sg} = 5 m/s show the best periodicity, It's indicated that the slug flow under this condition is relatively stable. As gas velocity increases to V_{sg} = 10 m/s of Figure (c), it's periodic frequency increases significantly compared with (a) and (b). Besides, the void fraction corresponding to the liquid slug (i.e. the concave part of a curve) increases from 0.1 of Figure (a) to 0.3 of Figure (c). It shows that under the condition of high gas velocity of 10 m/s, the liquid slug of slug flow becomes indistinct and is virtually permeated by the gas phase.

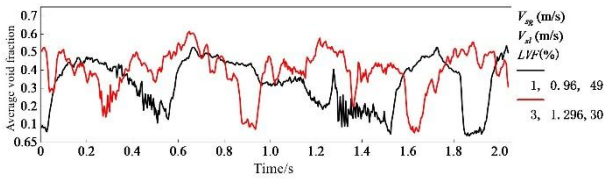

(a) Slug flow with low gas velocity

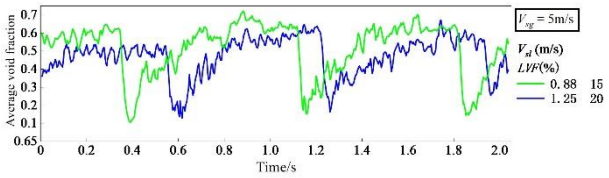

(b) Slug flow with V_{sg} = 5 m/s

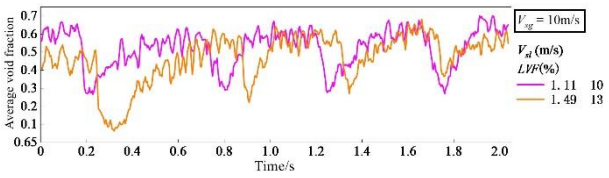

(c) Slug flow with V_{sg} = 10 m/s

Figure 6: Time series of the cross-sectional average void fraction

On the whole, the fluctuation range of the void fraction of the stratified flow is small, and its value stays almost the same, but the fluctuation frequency is the largest. The fluctuation amplitude of the void fraction of wavy flow is larger than that of stratified flow, and the fluctuation has certain randomness without obvious regular patterns. The fluctuation range of void fraction of slug flow is the largest among the three, and its fluctuation has a certain periodicity, which consists with the slug-flow characteristics of alternative flowing of gas slug and liquid slug.

4.2 PDFs of void fraction

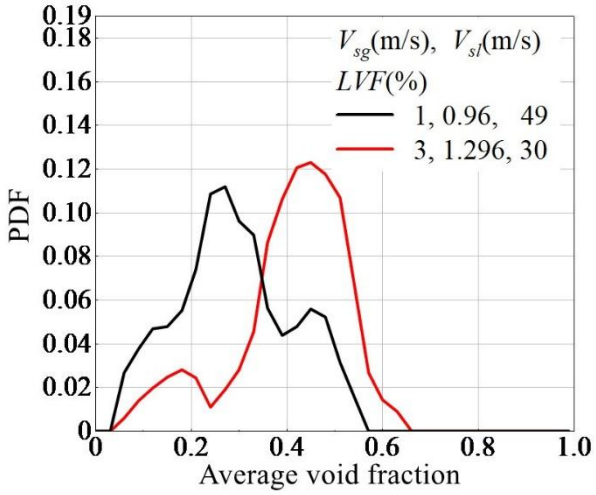

(a) Slug flow with low gas velocity

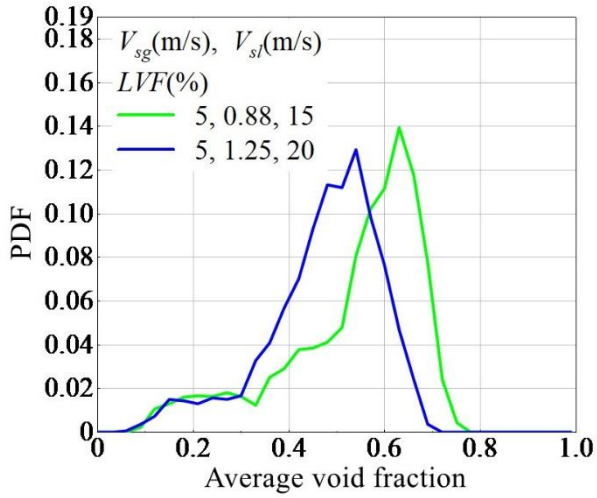

(b) Slug flow with V_{sg} = 5 m/s

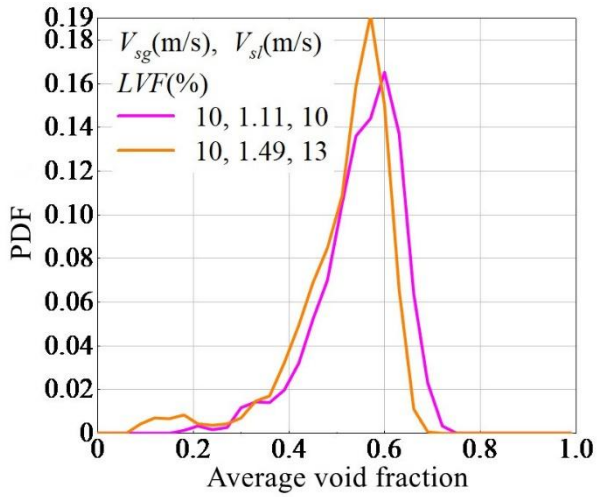

(c) Slug flow with V_{sg} = 10 m/s

Figure 7: PDFs of void fraction

Figure 7 is the PDFs of the void fraction of the slug flow under the condition of different gas velocity. The superficial gas velocity of Figure (a), Figure (b) and Figure (c) increases successively, which corresponds to the slug flow with slightly different fluid distributions.

The superficial gas velocity of Figure (a) is 1m/s and 3m/s respectively, and its PDFs shows a typical bimodal distribution. It including V_{sg} = 1m/s, V_{sl} = 0.96m /s, LVF = 49%, and V_{sg} = 3m/s, V_{sl} = 1.296m/s, LVF = 30%. The size relationship of the probability values corresponding the two peak points are opposite. It's indicated that the liquid phase is dominant phase under the former flowrate condition, on the contrary, the gas phase is dominant phase under the latter flowrate condition

In Figure (b) and Figure (c), the peak point corresponding to the smaller void fraction is not obvious. As the superficial gas velocity increases from 5 m/s of Figure (b) to 10 m/s of Figure (c), the probability value corresponding to the peak point with smaller void fraction decreases from 0.02 to 0. It's indicated that the percentage of the liquid slug has fallen under this condition. The liquid slug of Figure (c) almost disappears, where the PDFs of void fraction virtually shows a unimodal distribution. In Figure (b) and Figure (c), the peak point with to larger void fraction corresponds to the gas slug. It shows that the gas phase is the dominant phase of the slug flow with a relatively high gas velocity, and this peak point shifts to the right with the increase of the gas velocity, its corresponding probability value also increases.

The statistical results of the PDFs of the cross-sectional average void fraction shows that the probability values corresponding to the peak points of the slug flow are all small. The probability value corresponding to the lager peak points of Figure 7 (a) - (c) is 0.12, 0.13 and 0.18, respectively, all of them are smaller than the that of the stratified flow and the wavy flow.

5. Conclusion

In this paper, the experiments of gas-liquid two-phase slug flow measured by WMS are carried out and corresponding time series data are collected. From this, some measurement information such as the cross-sectional axial reconstructed images of fluid distribution and cross-sectional averaged void-fraction time series are obtained. On the basis of sampling data, the reconstruction of fluid distribution and the distribution characteristic of cross-sectional average void fraction time series are analyzed. The main conclusions are as follows:

(1) The flow experiments results of two-phase slug flow measured by WMS show that the normalized measurement has a good performance in the deriving of the reconstruction of phase distribution and the solution of the average void fraction. And the reconstruction of phase distribution completely consists with the time series of the cross-sectional average void fraction.

(2) The slug flow under different gas velocity presents three slightly different distribution patterns. when superficial gas velocity is less than 3 m/s, the gas phase mainly exists in the form of elongate gas slug. When superficial gas velocity is around 5 m/s, it appears as typical bullet-shape gas slug. As superficial gas velocity increases to 10 m/s, the liquid slug becomes blurred and the gas phase almost penetrates through the liquid slug structures.

(3) The PDFs of slug flow under condition of superficial gas velocity of 1- 3m/s show a typical bimodal distribution. As superficial gas velocity increases to middle or high velocity of 5-10 m/s, the probability value corresponding to the peak with smaller void fraction virtually decreases to 0, i.e. its PDFs almost show a unimodal distribution. The classification and discrimination of flow regimes can be realized by the PDFs of the cross-sectional average void-fraction time series.

References

[1] Prasser H M, Böttger A, Zschau J, "A new electrode-mesh tomograph for gas-liquid flows",

Flow Measurement and Instrumentation, 9(2),111-119, 1998.

[2] Prasser H M, Scholz D, Zippe C, “Bubble size measurement using wire-mesh sensors”, Flow Measurement and Instrumentation, 12(4), 299-312, 2001.

[3] Prasser H M, “Evolution of interfacial area concentration in a vertical air-water flow measured by wire-mesh sensors”, Nuclear Engineering and Design, 237,1608-1617, 2007.

[4] Joung O J, Kim Y H, Kim S P, “Measurement of gas velocity distribution using a wire-mesh electrostatic probe”, Sensors and Actuators A: Physical, 112, 237-243,2004.

[5] Kesana N R, Parsi M, Vieira R E, et al, “Visualization of gas-liquid multiphase pseudo-slug flow using Wire-Mesh Sensor”, Journal of Natural Gas Science and Engineering, 46(1), 477-490, 2017.

[6] Schleicher E, Besim Aydin T, Vieira R E, et al, “Refined reconstruction of liquid-gas interface structures for stratified two-phase flow using wire-mesh sensor”, Flow Measurement and Instrumentation, 46, 230-239, 2015.

[7] Richter S, Aritomi M, Prasser H M, et al, “Approach towards spatial phase reconstruction in transient bubbly flow using a wire-mesh sensor”, International Journal of Heat and Mass Transfer, 45(5), 1063-1075, 2002.

[8] Wangjiraniran W, Aritomi M, Kikura H, et al, “A study of non-symmetric air water flow using wire mesh sensor”, Experimental Thermal and Fluid Science, 29(3), 315-322, 2005.

[9] Prasser H M, Misawa M, Tiseanu I, “Comparison between wire-mesh sensor and ultra-fast X-ray tomograph for an air-water flow in a vertical pipe”, Flow Measurement and Instrumentation, 16, 73-83, 2005.

[10] Banowski, M, Beyer M, Szalinski L, et al, “Comparative study of ultrafast X-ray tomography and wire-mesh sensors for vertical gas–liquid pipe flows”, Flow Measurement and Instrumentation, 53, 95-106, 2017.

[11] Manera A, Ozar B, Paranjape S, et al, “Comparison between wire-mesh sensors and conductive needle-probes for measurements of two-phase flow parameters”, Nuclear Engineering and Design, 239(9), 1718-1724, 2009.